COMPDYN 2015
5th ECCOMAS Thematic Conference on
Computational Methods in Structural Dynamics and Earthquake Engineering
M. Papadrakakis, V. Papadopoulos, V. Plevris (eds.)
Crete Island, Greece, 25–27 May 2015

NONLINEARITY DETECTION AND IDENTIFICATION USING DISCRETE-TIME VOLTERRA SERIES: APPLICATION TO A SOLAR ARRAY STRUCTURE

Cristian Hansen[1,a], **Samuel da Silva**[1,b], **Emmanuel Foltête**[2,c] **and Scott Cogan**[2,d]

[1]UNESP - Univ Estadual Paulista, Faculdade de Engenharia de Ilha Solteira, Departamento de Engenharia Mecânica
Av. Brasil 56, 15385-000, Ilha Solteira, SP, Brasil
e-mail: [a]engcristianhansen@gmail.com, [b]samuel@dem.feis.unesp.br

[2] Université de Franche-Comté, Institut FEMTO-ST, Département Mécanique Appliquée
26, rue de l'Epitaphe - 25000 Besançon, France
e-mail: [c]emmanuel.foltete@femto-st.fr, [d]scott.cogan@univ-fcomte.fr

Keywords: nonlinearity detection, nonlinear system identification, Volterra series, panel structures

Abstract. *The aim of this paper is to identify a nonlinear model using time responses obtained from a sine sweep excitation applied to a simplified solar array structure. The nonlinearity is mainly caused by impacts, gaps and friction between the clamped interfaces of adjacent panels. A nonparametric model is identified using Volterra series, where the kernels are expanded with Kautz functions in order to decrease the problems associated with convergence and number of samples. The multiple convolutions provided by the Volterra kernels are used to propose a decision criterion based on a threshold limit to detect the level of linear or nonlinear behavior. The approach is also able to separate the linear and nonlinear contributions of the measured total response. The application performed in the experimental setup demostrates that the proposed method is successful in identifying the main nonlinear mechanism involved, despite of the complicated nature of the nonlinear system investigated.*

1 INTRODUCTION

Nonlinearities in healthy conditions is common in practice due to inherent nonlinear effects such as jumps, gaps, super harmonics, cycle limits, discontinuities, as well as others that appear frequently in the responses of structures [1]. This behavior is mainly due to excitation conditions, large displacements, geometric effects, nonlinear constitutive equations of the stress-strain etc [1–3]. Thus, the conventional linear procedures for structural analysis can fail when the system monitored is highly nonlinear in the healthy state [4, 5].

To illustrate these results, an experimental application is performed in a simplified test rig to simulate the complex dynamics of folded solar panels. The benchmark contains a snubber mounted with a small gap, that provides impacts under large displacements. The spatial mass distribution of the panels results in complex dynamics with many modal shapes in a small frequency bandwidth. The application of an excitation signal with energy in a small frequency bandwidth around the first resonance mode is expected to yield a single mode contribution in the response. However, impacts excite a large frequency bandwidth similar to an impact hammer test. Hence, several harmonics are excited due to coupling with high order modes. The biggest challenge is to separate the natural modal contribution from the contribution of the nonlinear behavior caused by the impacts. Several recent papers have investigated techniques to identify and to detect these effects [6, 7].

The Volterra series can be applied to solve this problem using its capability to decompose the response of a nonlinear system in linear and nonlinear contributions [8–12]. The contribution of the present paper is to propose a nonlinear indicator based on Volterra kernels to the detect the contribution of the linear and nonlinear kernels computed from the total experimental response measured directly on the solar array structure.

2 DISCRETE-TIME VOLTERRA SERIES

The response $y(k)$ of a nonlinear system is described by a discrete-time Volterra series using multiple convolutions [13]:

$$y(k) = \sum_{\eta=1}^{+\infty} \mathscr{H}_\eta(k) = y_1(k) + y_2(k) + y_3(k) + \cdots \tag{1}$$

where $y_1(k)$, $y_2(k)$, $y_3(k)$, $\cdots$ are the linear, quadratic, cubic and so on contributions of the output $y(k)$ in $k = 1, \cdots, K$ (K is the number of time samples) and $\mathscr{H}_\eta(k)$ is the Volterra functional given by multidimensional convolutions:

$$\mathscr{H}_\eta(k) = \sum_{n_1=0}^{N_1} \cdots \sum_{n_\eta=0}^{N_\eta} \mathcal{H}_\eta(n_1, \ldots, n_\eta) \prod_{i=1}^{\eta} u(k - n_i)$$

where $u(k)$ is the input signal and $\mathcal{H}_\eta(n_1, \ldots, n_\eta)$ are the η *th*-order Volterra kernels considering the truncated values $N_1, \ldots, N_\eta$ for each kernel.

However, the number of samples $N_1, \ldots, N_\eta$ is high because the practical systems have large memories and the identification of the kernels $\mathcal{H}_\eta(n_1, \ldots, n_\eta)$ is ill-posed with serious convergence problems. Fortunately, the Volterra kernels can be expanded using Kautz functions to overcome these drawbacks:

$$\mathcal{H}_\eta(n_1, \ldots, n_\eta) \approx \sum_{i_1=1}^{J_1} \cdots \sum_{i_\eta=1}^{J_\eta} \mathcal{B}_\eta\left(i_1, \ldots, i_\eta\right) \prod_{j=1}^{\eta} \psi_{i_j}(n_j) \tag{2}$$

where $J_1, \cdots, J_\eta$ are the number of samples in each orthonormal projections of the Volterra kernels $\mathcal{B}_\eta(i_1, \ldots, i_\eta)$ and and $\psi_{i_j}(n_i)$ are the Kautz functions that are appropriate for the representation of underdamped oscillatory systems.

If the Kautz basis is chosen adequately the order of projection $\mathcal{B}_\eta(i_1, \ldots, i_\eta)$ is drastically reduced [10]. Details about the Kautz functions and how to use it for nonlinear mechanical systems identification can be found in [14] and [9].

Equation (1) can be rewritten based on the orthonormal Kautz basis:

$$y(k) \approx \sum_{\eta=1}^{+\infty} \mathscr{B}_\eta(k) \tag{3}$$

where $\mathscr{B}_\eta(k)$ is the $\eta-th$ orthonormal Volterra functional operator:

$$\mathscr{B}_\eta(k) \approx \sum_{i_1=1}^{J_1} \cdots \sum_{i_\eta=1}^{J_\eta} \mathcal{B}_\eta(i_1, \ldots, i_\eta) \prod_{j=1}^{\eta} l_{i_j}(k)$$

that is a multiple convolution between the orthonormal kernel given by $\mathcal{B}_\eta(i_1, \ldots, i_\eta)$ and $l_{i_j}(k)$, that is a simple filtering of input signal $u(k)$ by the Kautz function $\psi_{i_j}(n_i)$:

$$l_{i_j}(k) = \sum_{n_i=0}^{V-1} \psi_{i_j}(n_i) u(k - n_i) \tag{4}$$

where $V = \max\{J_1, \ldots, J_\eta\}$ and $\psi_{i_j}(n_i)$ are the Kautz functions described by complex-conjugate parameters $s_{1,2} = -\xi_\eta \omega_\eta \pm j\omega_\eta \sqrt{1 - \xi_\eta^2}$. Normally, an optimization procedure is used to obtain the parameters ω_η, ξ_η.

The values of the orthonormal Volterra kernel $\mathcal{B}_\eta(i_1, \ldots, i_\eta)$ can be grouped in a vector $\mathbf{\Phi}$ and can be found by solving:

$$\mathbf{\Phi} = (\mathbf{\Gamma}^T \mathbf{\Gamma})^{-1} \mathbf{\Gamma}^T \mathbf{y} \tag{5}$$

where the matrix $\mathbf{\Gamma}$ contains $l_{i_j}(k)$ and $\mathbf{y} = [y(1) \cdots y(K)]$. It is worth noting that η can usually be truncated in 3 kernels to represent most of the structural nonlinearities with a smooth behavior.

The prediction error can be computed by:

$$e(k) = y(k) - y_{exp}(k) \tag{6}$$

where $y_{exp}(k)$ is the experimental output and $y(k)$ is the output estimated by Volterra model.

The complex-conjugate parameters of the Kautz functions are obtained by minimizing the normalized mean square error-prediction (NMSE):

$$\min \quad F = \frac{||e(k)||_2}{||y_{exp}(k)||_2} \tag{7}$$

subject to $\boldsymbol{\rho}_{low} \leq \boldsymbol{\rho} \leq \boldsymbol{\rho}_{up}$, where the Kautz filters parameters (using $\eta = 3$) grouped in the vector $\boldsymbol{\rho} = [\omega_1 \ \xi_1 \ \omega_2 \ \xi_2 \ \omega_3 \ \xi_3]^T = [\omega_{lin} \ \xi_{lin} \ \omega_{quad} \ \xi_{quad} \ \omega_{cub} \ \xi_{cub}]^T$ and $||\ ||_2$ is the Frobenius norm, also called the Euclidean norm.

The vectors $\boldsymbol{\rho}_{low}$ and $\boldsymbol{\rho}_{up}$ are composed by the lower and upper boundary values of search. This work adopted a sequential quadratic programming (SQP) approach to seek the vector $\boldsymbol{\rho}$ using an initial condition vector $\boldsymbol{\rho}_0$.

3 APPLICATION IN A SOLAR ARRAY STRUCTURE

This section shows an experimental application of the methodology using a simplified solar array structure [6, 7].

3.1 Description of the experimental setup

The benchmark consists of two parallel aluminium plates mounted in a free-free configuration, as seen in Figures 1(a) and 1(b). They are clamped together at the top edge and connected at three stacking points. The geometrical properties of the plates are $770 \times 440 \times 5$ mm of, length, width and thickness, respectively, and the distance between plates is fixed at 40 mm.

A snubber was also mounted on a steel support glued at the middle length of the bottom free edge, as shown in Figures 1(a), 1(b) and 2(a). When the level of excitation amplitude applied in the shaker is high, the rubber exhibits nonlinear behavior and impacts between the adjacent panels. As pointed out in Ref. [6], the small contact areas between the stacking points and the plates are an additional possible source of non-linear behavior, as they may induce large, localized bending deformations. In this study, a gap of less than one millimeter (≈ 0.2 mm) is introduced such that there is no contact when the level of force is low in order to insure a linear regime of vibration (see Figure 2(a)).

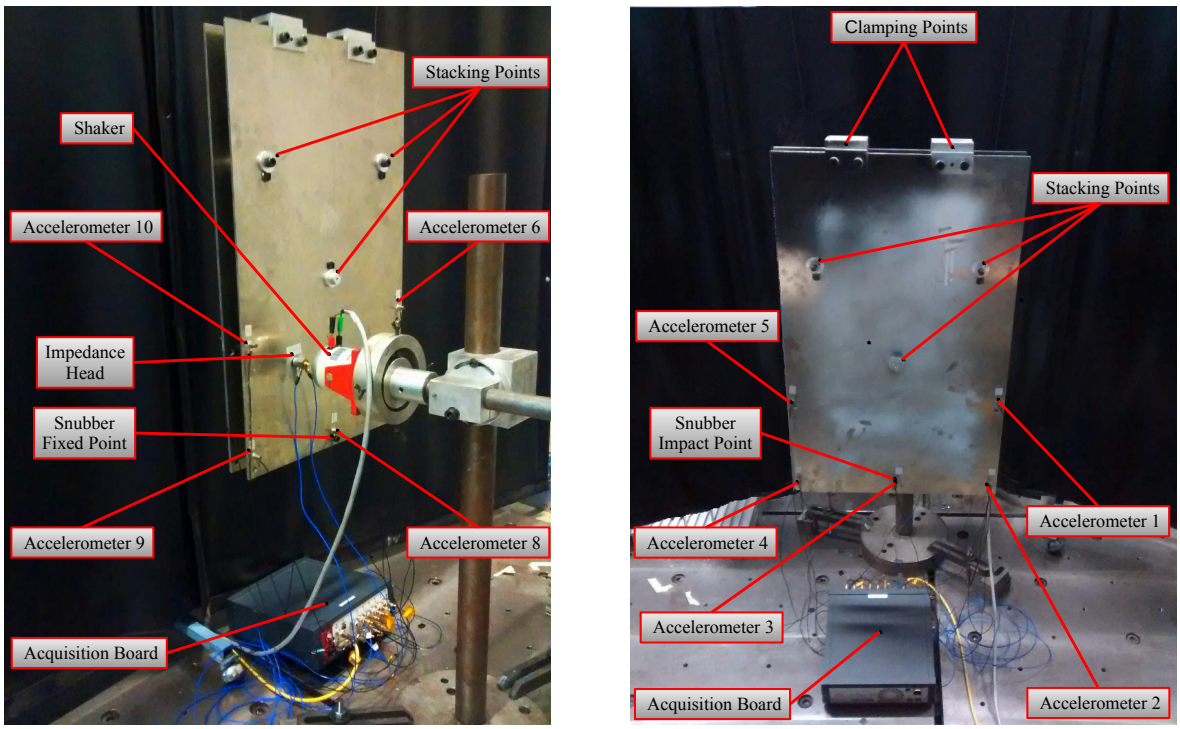

(a) Experimental setup. (b) Detail of the experimental setup.

Figure 1: Test rig setup.

The structure was monitored using 10 accelerometers, 5 on each plate at the same positions. In this work, only the measurements at accelerometer 3, mounted in the impact region of the target plate, were used. An impedance head was also employed to measure the drivepoint accelerations and the excitation force. All signals measured were sampled at 1280 Hz, 6400 samples for tests with short duration (to identification and analysis) and 256000 samples for tests with long duration (to characterize the nonlinear behavior). In order to remove the contribution from the high order modes and DC component, a bandpass filter was applied from 5 to 120 Hz.

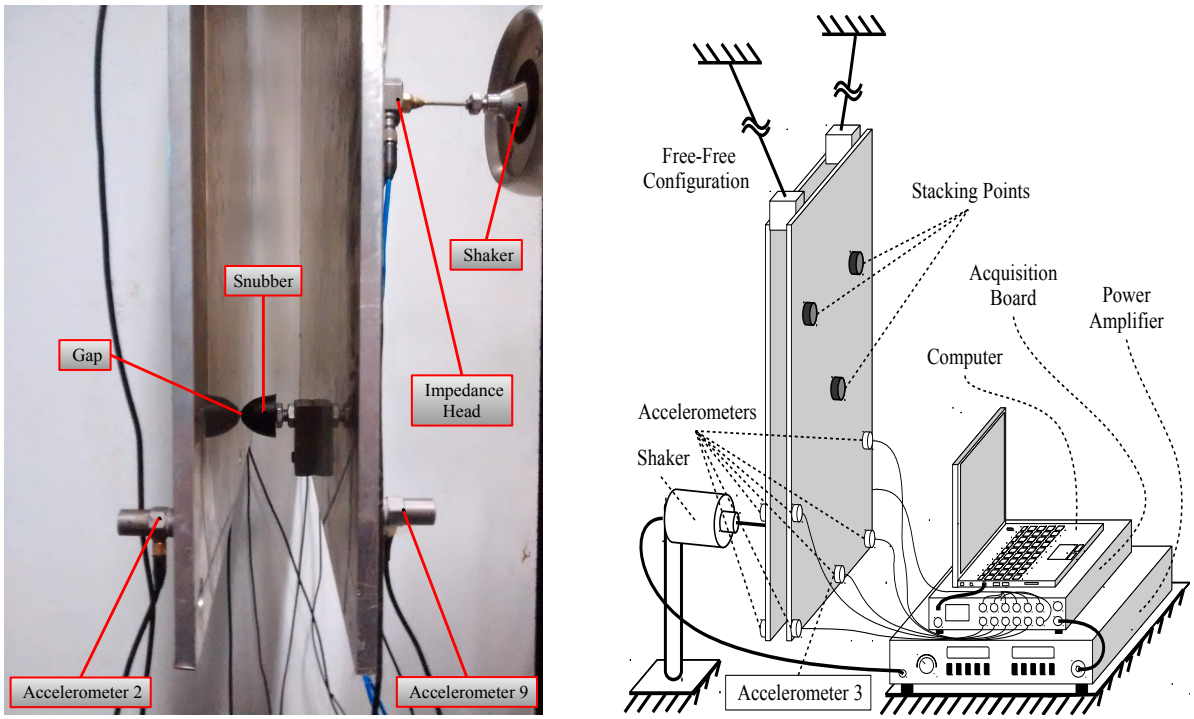

(a) Zoom in the impact region, showing the snubber.

(b) Schematic representation.

Figure 2: Description of the experimental setup.

3.2 Detection of nonlinearities using classical methods

The stepped sine test is an effective tool to detect nonlinear behavior. But an alternative and easier test is to excite the system with a long duration sweep sine. Figure 3 shows the acceleration considering low (fig. 3(a)) and high (fig. 3(b)) voltage amplitude supplied to the shaker. In all cases the sine sweep is applied ranging the frequency from 10 to 45 Hz during 200 seconds. Figure 3(a) shows a smooth decay after resonance (linear vibration). However, fig. 3(b) presents two differences: a jump is observed close to the frequency of 36.25 Hz and the resonance frequency is changed.

Figures 3(a) and 3(b) show the maximum amplitude of the time of flight (TOF). Figure 4(a) presents the ratio between the time and excitation frequency to estimate the output frequency of TOF. When the energy[1] of the force excitation is low, the TOF occurs at the same frequency, both in upward and downward sine sweep tests. However, when the force is increased, the resonance frequency is bigger following a sigmoid ratio as a function of the applied energy. Another important issue is that this behavior is different depending the type of sweep test. This is a clear indication of the existence of nonlinearities.

Figure 4(b) shows the frequency response function (FRF) plots. The FRFs show some distortions caused by nonlinear effects as a function of force level applied by the shaker. By analyzing Figure 4(b) it is possible to confirm that the solar array structure presents a strong nonlinear regime of motion associated with stiffness hardening that cause a jump on the right side.

Figures 5(a) and 5(b) show the time-frequency distribution considering the acceleration signal in the upward and downward sweep tests, respectively. One can observe the first three harmonics caused by impacts and large displacements, mainly in the resonance range.

[1]Computed by $L2$ norm.

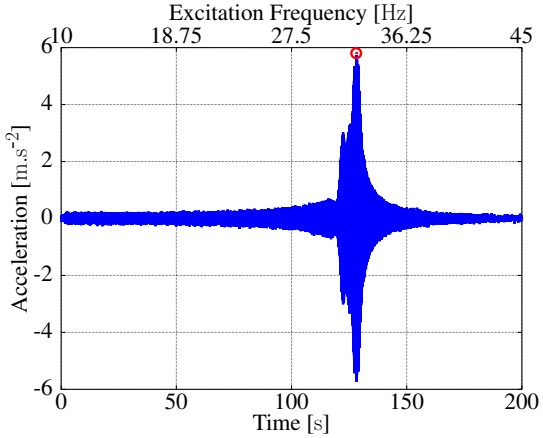

(a) Low excitation amplitude level (0.01 V).

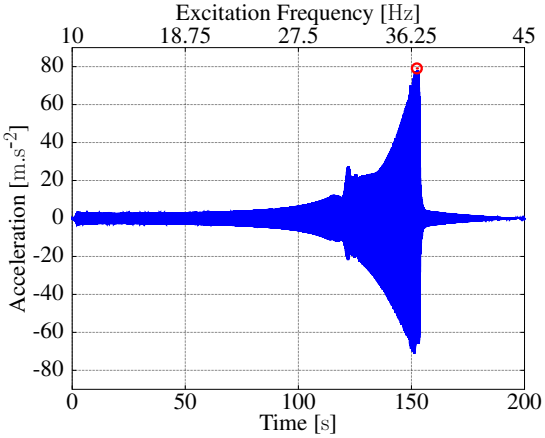

(b) High excitation amplitude level (0.20 V).

Figure 3: Output to sine sweep with frequency from 10 to 45 Hz considering different voltage amplitudes applied in the shaker. The maximum amplitude of the time of flight is represented by ○.

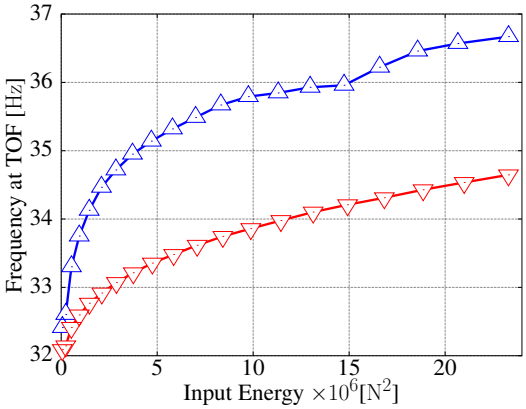

(a) Frequency at TOF, the marker △ represents the sine sweep up (10→45 [Hz]) and the marker ▽ represents the sine sweep down (45→10 [Hz]).

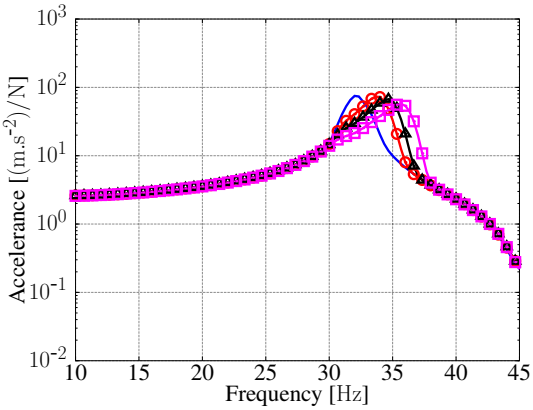

(b) Accelerance, in continous line — for (0.03 V), ○ for (0.08 V), △ for (0.12 V) and □ for (0.20 V).

Figure 4: Frequency at TOF and FRF estimated using the sine sweep test with long duration.

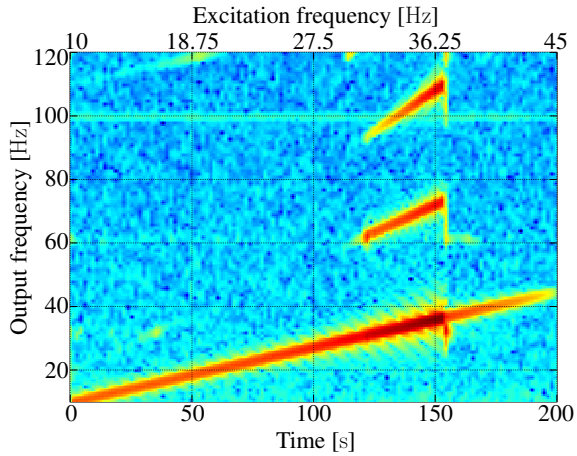

(a) Sine sweep up test, 10→45 Hz.

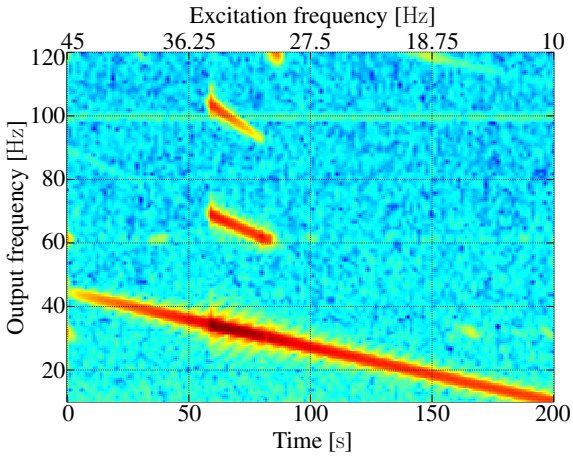

(b) Sine sweep down test, 45→10 Hz.

Figure 5: Time-frequency distribution of the acceleration signal considering the high level of amplitude excitation, 0.20 V.

3.3 Identification of the Volterra model

The identification of the Volterra kernels is performed using the sine sweep signal in two steps [11]. Firstly, the kernel $\mathcal{H}_1(n_1)$ is identified to describe the linear contribution. Secondly, the high order kernels $\mathcal{H}_2(n_1, n_2)$ and $\mathcal{H}_3(n_1, n_2, n_3)$ are identified using the response signal filtered by $\mathcal{H}_1(n_1)$ estimated previously. All parameters in the Kautz functions are used based on the optimization procedure described in [9, 15].

A total of 30 blocks were measured with 6400 samples each for 20 different levels of voltage amplitude applied in the shaker. Disturbances are included in the excitation signal by changing 12^{o} in each block (360^{o} total).

The choice of the number of Kautz functions can be complicated for structures with strong nonlinear effects and in this work with high order modes excitated by impacts. For the first kernel, a couple of Kautz functions is enough to adequately describe the linear behavior of a single degree-of-freedom system, based on previous experience using the Volterra series [12, 16–26]. The second kernel is related essentially to asymmetries in the response appearing as second harmonics in the time-frequency distribution. However, shaker-structure interaction can result mainly in a second harmonic excitation.

For the third kernel an optimization procedure can show the best number of Kautz functions to use, but the choice here was limited to 6 Kautz functions because of convergence problems trying solve a high order equation using more functions. So, the Volterra model was estimated for each test, using 2, 4 and 6 Kautz functions for $\mathcal{H}_1(n_1)$, $\mathcal{H}_2(n_1, n_2)$ and $\mathcal{H}_3(n_1, n_2, n_3)$, respectively.

The Kautz filter parameters used to build the orthonormal kernels were found with a sequential quadratic programming (SQP) algorithm minimizing the objective function F in Eq. (7) with the stopping criterion based on a step size less than 10^{-8}.

The initial condition vector $\boldsymbol{\rho_0}$ for the low excitation amplitudes applied on the shaker (0.01 V) was defined as $\boldsymbol{\rho_0} = [\omega_0 \;\; \xi_0 \;\; \omega_0 \;\; \xi_0 \;\; \omega_0 \;\; \xi_0]$, where ω_0 is the resonant frequency computed by the fast Fourier transform of $y_{exp}(k)$ for the low amplitude level (0.01 V) and $\xi_0 = 10^{-3}$. For the all other amplitudes levels, the initial condition vector is computed by:

$$\boldsymbol{\rho}_0 = \frac{1}{N} \sum_{i=1}^{N} {}_i\boldsymbol{\rho}^* \tag{8}$$

where N is the number of blocks for each level of amplitude applied in the shaker ($N = 30$) and ${}_i\boldsymbol{\rho}^*$, $i = 1, 2, 3, \ldots N$, is the optimum value vector for each block of the immediately lower amplitude level.

The lower and upper boundary values of the search was defined by:

$$\boldsymbol{\rho}_{low} = \left[\begin{array}{cccccc} 0.8\boldsymbol{\rho}_0(1) & 0 & 0.8\boldsymbol{\rho}_0(3) & 0 & 0.8\boldsymbol{\rho}_0(5) & 0 \end{array} \right] \tag{9}$$

$$\boldsymbol{\rho}_{up} = \left[\begin{array}{cccccc} 1.2\boldsymbol{\rho}_0(1) & 1 & 1.2\boldsymbol{\rho}_0(3) & 1 & 1.2\boldsymbol{\rho}_0(5) & 1 \end{array} \right] \tag{10}$$

The fitness (FIT $= F^{-1} \times 100$ [%]) of the optimization procedure is shown in Figure 6. A bigger fit is reached when the vibration is linear (amplitudes from 0.02 to 0.06 V). When the level of force increases, the fit is poor (amplitudes from 0.08 to 0.20 V) because the model is insufficent to detect the large nonlinear behavior caused by coupling with the high order modes.

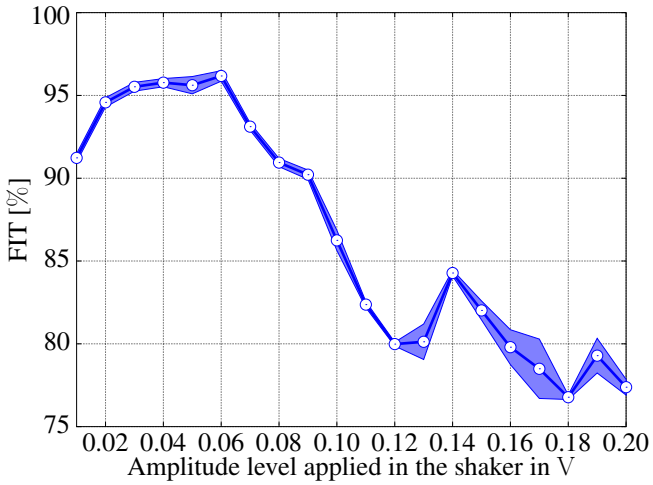

Figure 6: Fitness values lie within one standard deviation of the mean for each test.

The parameters, frequency and damping ratio, of Kautz poles related with each Volterra kernel are shown in Figures 7, 8 and 9. The values are seen to lie within one standard deviation of the mean. In a broader view, all parameters, with the exception of ξ_{quad}, are increasing with the levels of amplitude applied to the shaker, showing that the impacts are changing the structural behavior constantly following the excitation levels.

Figure 7(a) presents the same frequency, ω_{lin}, for low levels of amplitude applied in the shaker (up to level 0.07 V). The damping ratio, ξ_{lin}, of the Kautz poles are increased by the impacts that occur with the levels up to 0.05 V, as shown in Figure 7(b).

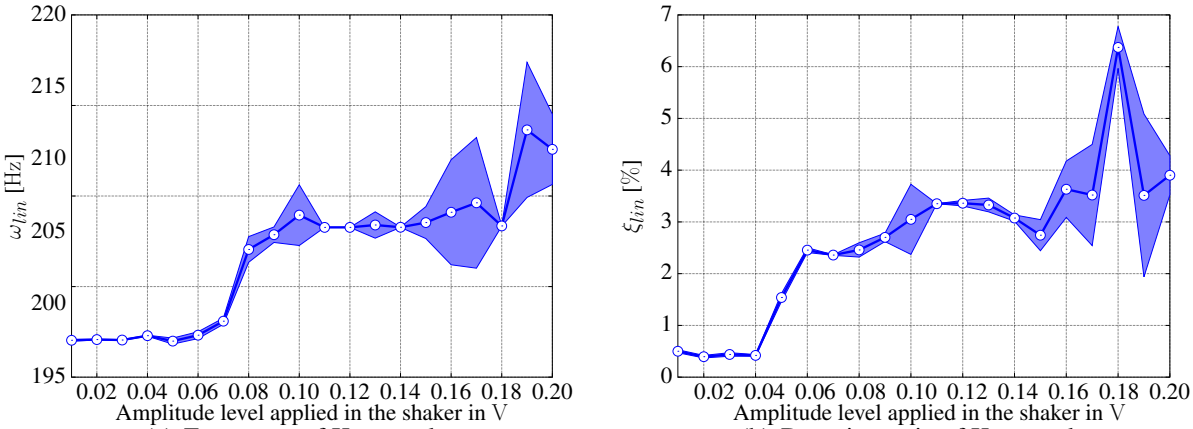

(a) Frequency of Kautz poles.

(b) Damping ratio of Kautz poles.

Figure 7: Kautz poles of $\mathcal{H}_1(n_1)$, values lie within one standard deviation of the mean for each test.

The high order kernels do not have significant contributions at low levels of excitation since the behavior is linear. Hence, if the second and third kernels are included in the identification process at low amplitudes then the results are not consistent because the system is essentially linear. Figure 8(b) confirms that for the levels up to 0.05 V the poles are highly damped with null contributions in the high order kernels. The frequency of the Kautz poles in the second kernel increases with the level of excitation, as shown in Figure 8(a). This effect is caused by the shaker-structure interaction in the resonance range of the system.

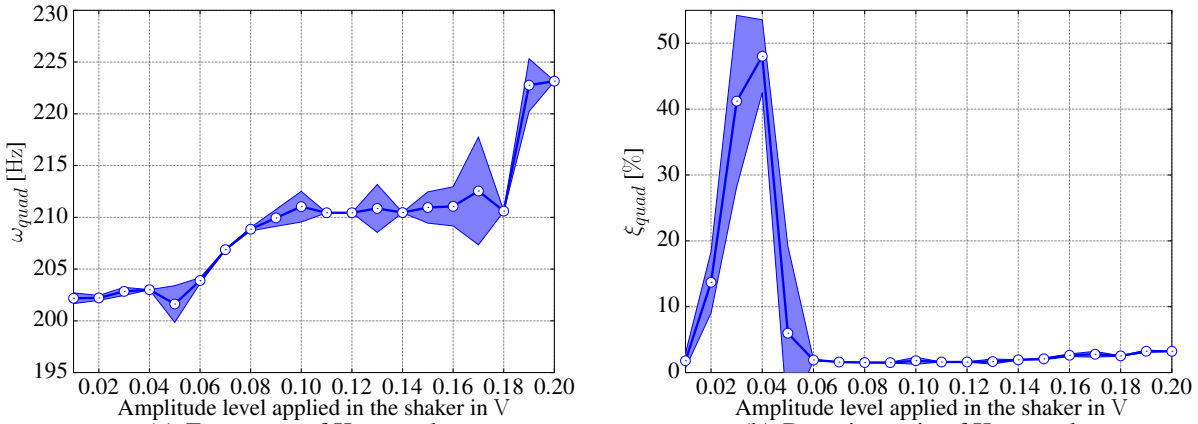

(a) Frequency of Kautz poles. (b) Damping ratio of Kautz poles.

Figure 8: Kautz poles of $\mathcal{H}_2(n_1, n_2)$, values lie within one standard deviation of the mean for each test.

Figure 9(a) and 9(b) show the evolution of the Kautz pole parameters, frequency and damping ratio, for the third kernel. Similar behavior is found, except in the range from 0.10 to 0.13 V in the damping ratio.

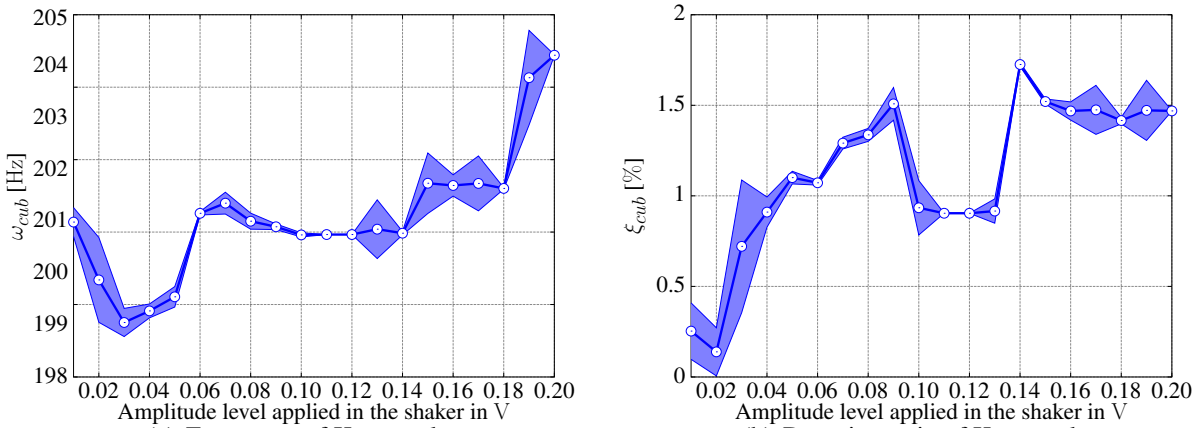

(a) Frequency of Kautz poles. (b) Damping ratio of Kautz poles.

Figure 9: Kautz poles of $\mathcal{H}_3(n_1, n_2, n_3)$, values lie within one standard deviation of the mean for each test.

Figure 10(a) shows the estimated output obtained by the multiple convolution computed using the Volterra kernels $\mathcal{H}_1(n_1)$, $\mathcal{H}_2(n_1, n_2)$ and $\mathcal{H}_3(n_1, n_2, n_3)$ for the excitation level 0.01 V applied in the shaker. The prediction error computed by Eq. (6) is shown in Figure 10(b). The second and third kernels, $\mathcal{H}_2(n_1, n_2)$ and $\mathcal{H}_3(n_1, n_2, n_3)$, respectively, do not have a significant contribution to the linear behavior and the response of the Volterra model, $y(k)$, for this case (linear behavior) can be approximated using only the linear contribution, $y_1(k)$.

When the amplitude level applied in the shaker is high, the nonlinear vibrating regime is reached and the nonlinear contributions, $y_2(k)$ and $y_3(k)$ have importance in the total response, $y(k)$. Figure 11(a) shows the output identified by the Volterra model for high amplitude level applied in the shaker and Figure 11(b) the prediction error to this condition.

Figures 12, 13 and 14 present the linear, quadratic and cubic contributions of the total response when the amplitude level is 0.20 V. It is worth noting that the quadratic contribution is lower than the linear contribution because the symmetry of the output signal, as shown in Figure 13. On the other hand, when the level excitation is high, the cubic contribution is significant in comparison to the linear response, as shown in Figure 14.

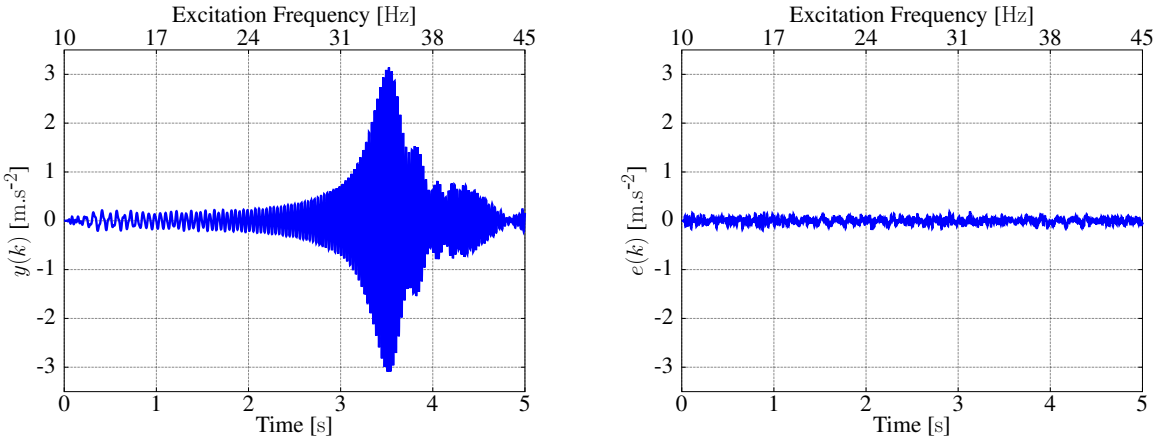

(a) Estimated output by the Volterra model. (b) Prediction error.

Figure 10: Output for the low level amplitude (0.01 V).

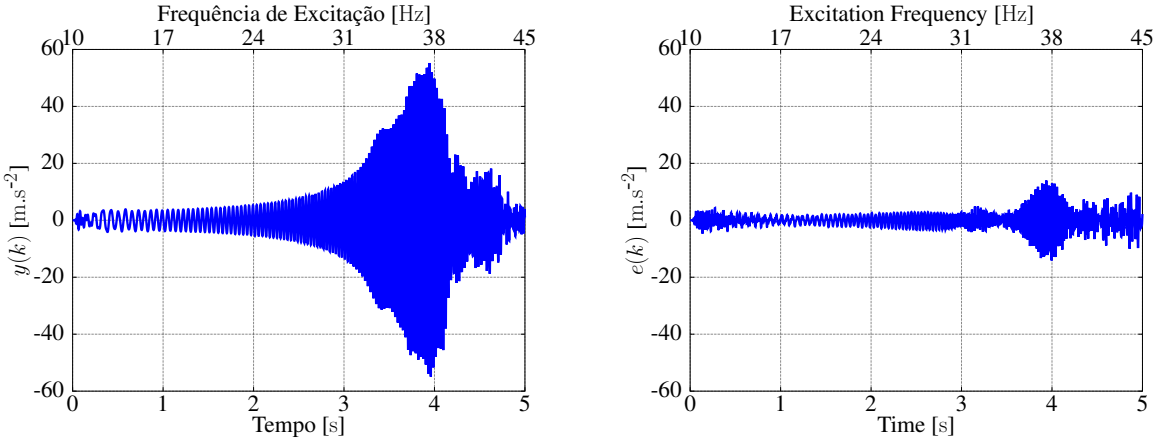

(a) Estimated output by the Volterra model. (b) Prediction error.

Figure 11: Output for the high level amplitude (0.20 V).

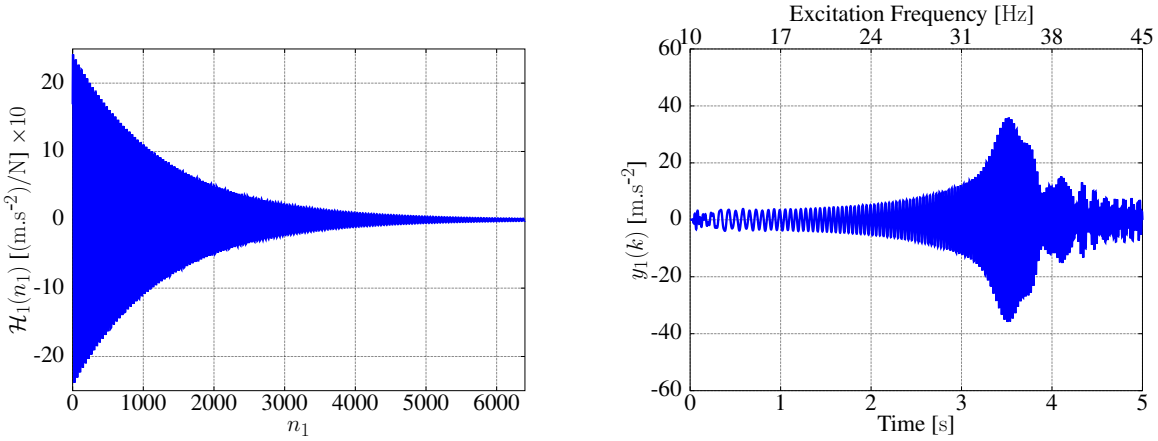

(a) Volterra kernel $\mathcal{H}_1(n_1)$. (b) $y_1(k)$ estimated by $\mathcal{H}_1(n_1)$.

Figure 12: Linear contribution considering 0.20 V of amplitude applied in the shaker.

The diagonal of the second kernel, $\mathcal{H}_2(n_1, n_1)$, is show in Figure 13(a) and its contribution, $y_2(k)$, was estimated by quadratic convolution, as shown in Figure 13(b). We note that the quadratic contribution is smaller than the linear contribution because of the symmetry in the response.

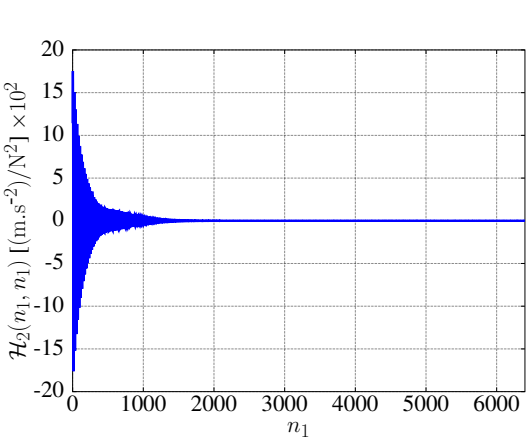

(a) Diagonal of Volterra Kernel $\mathcal{H}_2(n_1, n_2)$.

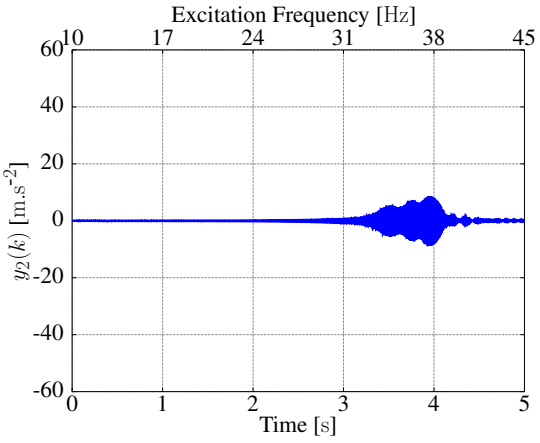

(b) $y_2(k)$ estimated by $\mathcal{H}_2(n_1, n_2)$.

Figure 13: Quadratic contribution considering 0.20 V of amplitude applied in the shaker.

The diagonal of the third kernel, $\mathcal{H}_3(n_1, n_1, n_1)$, is shown in Figure 14(a) and its contribution, $y_3(k)$, was computed by cubic convolution, as shown in Figure 14(b). The cubic contribution have the same level of significance in the total response when compared with the linear contribution.

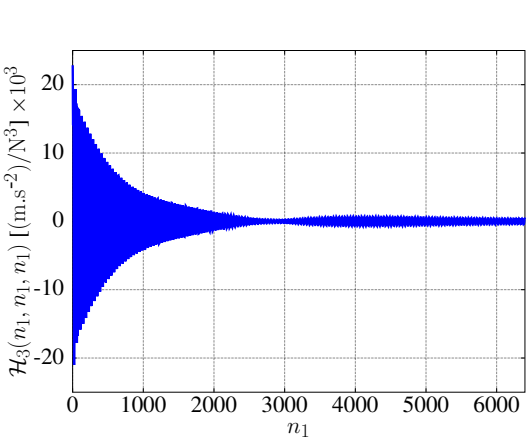

(a) Diagonal of Volterra kernel $\mathcal{H}_3(n_1, n_2, n_3)$.

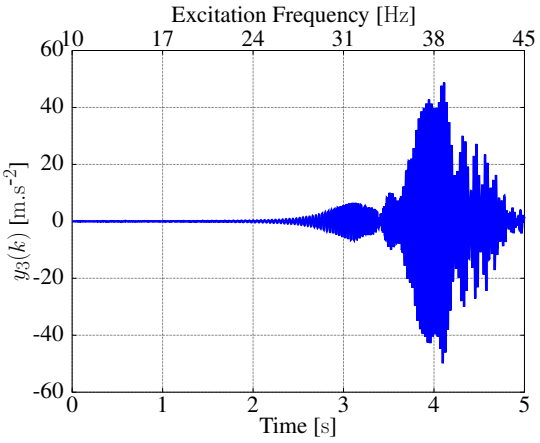

(b) $y_3(k)$ estimated by $\mathcal{H}_3(n_1, n_2, n_3)$.

Figure 14: Cubic contribution considering 0.20 V of amplitude applied in the shaker.

For high levels of amplitude applied in the shaker, the nonlinear contributions, $y_2(k)$ and $y_3(k)$, are relevant comparing with the total response, $y(k)$. So, compute the nonlinear contributions is necessary to obtain a representative model of a structure with nonlinear behavior.

3.4 Model Validation

The Volterra model identified was validated through the qualitative analysis of the time-frequency distribution of the acceleration signal considering the high level of amplitude excitation applied in the shaker, 0.20 V, as shown Figures 15(a) and 15(b).

Figure 16 also presents the validation of the FRF computed using the output estimated by Volterra model comparing with experimental FRF. It is possible to observe a good fit in the resonance range for the different levels of amplitude applied in the shaker.

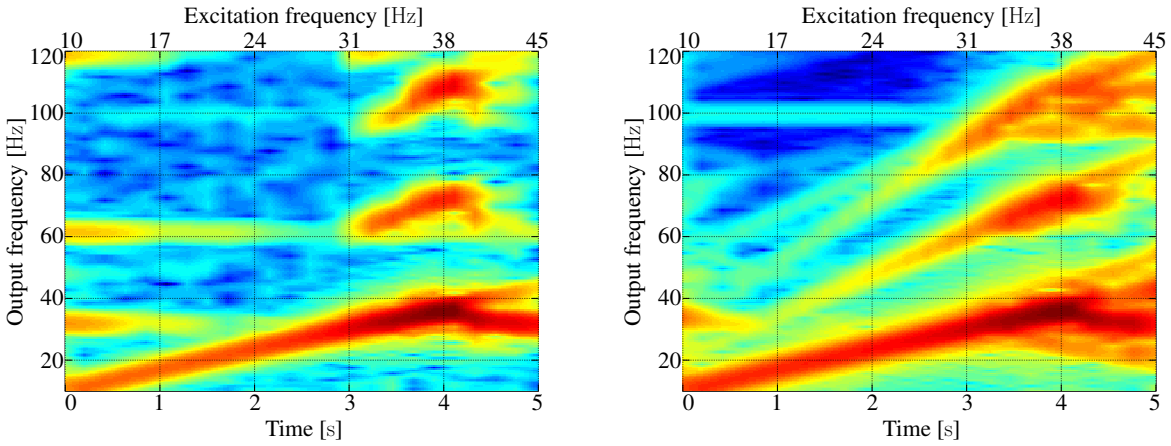

(a) Experimental. (b) Volterra model.

Figure 15: Time-frequency of the accelaration signal for the level of 0.2 V.

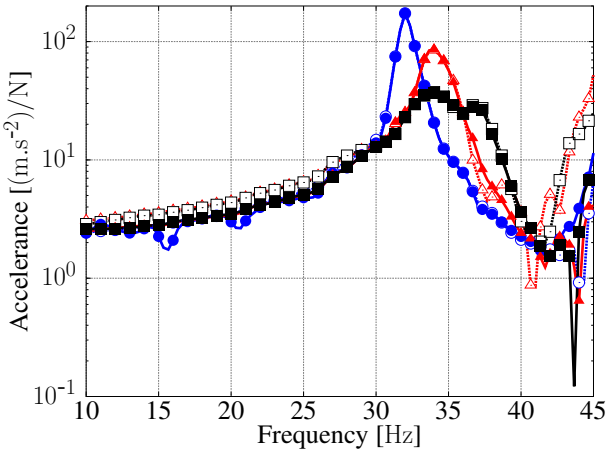

Figure 16: Frequency response function computed for a Volterra model response and experimental data. ● for the experimental and ○ for the model considering 0.01 V, ▲ for the experimental and △ for the model considering 0.10 V, ■ for the experimental and □ for the model considering 0.20 V.

3.5 Nonlinear index based in Volterra model

The output energy ratio κ can be described by using each contribution of the Volterra model:

$$\kappa = \frac{E_\alpha}{E_1 + E_2 + E_3};\ \alpha = 1, 2, 3 \tag{11}$$

where, E_1, E_2 and E_3 are the energy of linear, quadratic and cubic contributions, respectively, computed by $L2$ norm.

Figure 17, shows the κ for each Volterra contribution for all excitation amplitudes tested.The indicator shows that until the level of 0.04 V the linear contribution is dominant. After 0.04 V the energy contribution of the cubic stiffness caused by the third Volterra kernel starts to dominate. It is worth noting that the quadratic contribution is null for all levels.

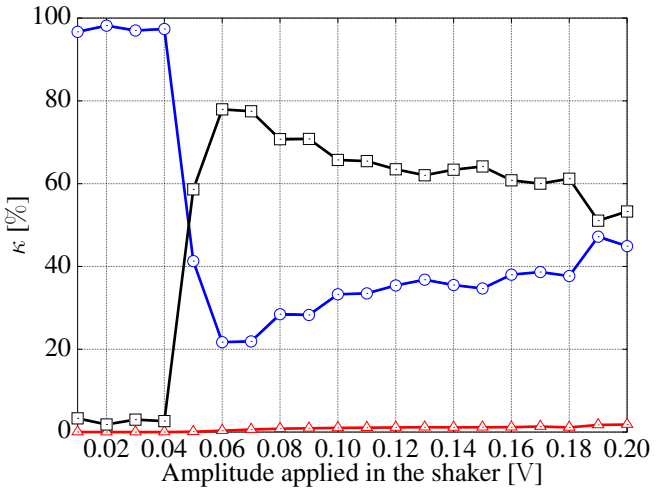

Figure 17: Indicator to detect nonlinearities based on the Volterra kernel contributions. ○ is the linear ratio, △ is the quadratic and □ is the cubic contribution.

4 FINAL REMARKS

The results of this study show that the use of Volterra series can identify a nonparametric model capable of describing the complex dynamic behavior of a solar array structure using directly the time domain data obtained for different excitation amplitudes and vibration regimes. The kernels identified can be used to filter the linear and nonlinear contributions and to compute an indicator for detecting nonlinearity. Future studies will consider a larger range of modal contributions with more kernels for each mode. The multiple inputs and multiple output cases can also be investigated using the Volterra cross-kernels.

5 ACKNOWLEDGMENTS

The authors acknowledge the financial support provided by Research Foundation of São Paulo (FAPESP, Brasil) through the grant number 12/09135-3 and the National Council for Scientific and Technological Development (CNPq, Brasil) through the grant number 470582/2012-0. The first author is thankful to FAPESP for his scholarship grants 13/09008-4 and 14/02431-1. The first and the second authors would like to thank the kind hospitality of Prof. Emmanuel Foltête and Scott Cogan during their stay in Besançon in 2014.

REFERENCES

[1] Gaëtan Kerschen, Keith Worden, Alexander F. Vakakis, and Jean-Claude Golinval. Past, present and future of nonlinear system identification in structural dynamics. *Mechanical Systems and Signal Processing*, 20(3):505 – 592, 2006.

[2] Keith Worden and G. R. Tomlinson. *Nonlinearity in Structural Dynamics - Detection, Identification and Modelling*. Institute of Physics Publishing, London, United Kingdom, 1 edition, 2001.

[3] L.N. Virgin. *Introduction to Experimental Nonlinear Dynamics: A Case Study in Mechanical Vibration*. Cambridge University Press, Cambridge, United Kingdom, 1 edition, 2000.

[4] C. R. Farrar, K. Worden, M. D. Todd, G. Park, J. Nichols, D. E. Adams, M. T. Bement, and K. Farinholt. Nonlinear system identification for damage detection. Technical Report LA-14353, Los Alamos National Laboratory (LANL), 2007.

[5] Keith Worden, Charles R. Farrar, Jonathan Haywood, and Michael Todd. A review of nonlinear dynamics applications to structural health monitoring. *Structural Control and Health Monitoring*, 15(4):540–567, 2008.

[6] A. Hot, G. Kerschen, E. Foltête, and S. Cogan. Detection and quantification of non-linear structural behavior using principal component analysis. *Mechanical Systems and Signal Processing*, 26(0):104 – 116, 2012.

[7] J.P. Noël and G. Kerschen. Frequency-domain subspace identification for nonlinear mechanical systems. *Mechanical Systems and Signal Processing*, (0):91–102, 2013.

[8] W. J. Rugh. *Nonlinear System Theory - The Volterra/Wiener Approach*. The Johns Hopkins University Press, 1991.

[9] Samuel da Silva, Scott Cogan, and Emmanuel Foltête. Nonlinear identification in structural dynamics based on Wiener series and Kautz filters. *Mechanical Systems and Signal Processing*, 24(1):52 – 58, 2010.

[10] Samuel da Silva. Non-linear model updating of a three-dimensional portal frame based on Wiener series. *International Journal of Non-Linear Mechanics*, 46(1):312 – 320, 2011.

[11] W. Silva. Identification of nonlinear aeroelastic systems based on the Volterra theory: Progress and opportunities. *Nonlinear Dynamics*, 39(1-2):25–62, 2005.

[12] Sidney Bruce Shiki, V. Lopes Jr, and S. da Silva. Damage detection in nonlinear structures using discrete-time Volterra series. *Key Engineering Materials*, 569-570:876–883, 2013.

[13] M. Schetzen. *The Volterra and Wiener theories of nonlinear systems*. New York: Wiley, 1980.

[14] Samuel da Silva. Non-parametric identification of mechanical systems by Kautz filter with multiple poles. *Mechanical Systems and Signal Processing*, 25(4):1103 – 1111, 2011.

[15] Sidney Bruce Shiki, V. Lopes Jr, and Samuel da Silva. Identification of nonlinear structures using discrete-time Volterra series. *Journal of the Brazilian Society of Mechanical Sciences and Engineering*, pages 1–10, 2013.

[16] S. B. Shiki, Jean-Philippe Noël, Gaëtan Kerschen, V. Lopes Jr, and S. da Silva. Identification of mechanical systems with local nonlinearities through discrete-time Volterra series and Kautz functions. In *11th International Conference on Recent Advances in Structural Dynamics - RASD 2013*, Pisa, Italy, 2013.

[17] Cristian Hansen, Luís Gustavo G. Villani, and S. da Silva. Aplicação de séries de Volterra na detecção de danos em uma viga com comportamento não-linear. In *VIII Congresso Nacional de Engenharia Mecânica - CONEM 2014*, Uberlândia, Brasil, August 2014.

[18] Cristian Hansen, Sidney Bruce Shiki, and S. da Silva. Non-parametric identification of a non-linear buckled beam using discrete-time Volterra series. In *9th International Conference on Structural Dynamics - Eurodyn 2014*, pages 2013–2018, Porto, Portugal, June-July 2014.

[19] Cristian Hansen, Sidney Bruce Shiki, and Samuel da Silva. Structural health monitoring in a buckled beam using volterra serie. In Vincent Le Cam, Laurent Mevel, and Franck Schoefs, editors, *7th European Workshop on Structural Health Monitoring (EWSHM 2014)*, Nantes, France, July 2014. IFFSTTAR, Inria, Université de Nantes.

[20] O. Scussel, G. J. Q. Vasconcelos, S. B. Shiki, and S. da Silva. Identification of mechanical systems through Volterra series - study of benchmark cases. In *Conferência Brasileira de Dinâmica, Controle e Aplicações (DINCON 2013)*, Fortaleza, CE, October 2013.

[21] S. da Silva. Damage detection in a 2 dof nonlinear mechanical systems using Volterra series and Kautz filter. In *20th International Congress of Mechanical Engineering (COBEM 2009)*, Gramado, Brasil, 2009. ABCM, UFRGS.

[22] S. B. Shiki, V. Lopes Jr, and S. da Silva. Identification of parameters in nonlinear structures using discrete Volterra series. In *IV Symposium on Intelligent Materials and Control*, 2012.

[23] Sidney Bruce Shiki, S. da Silva, and V. Lopes JR. Nonlinear mechanical systems identification through Wiener/Volterra series. In *22nd International Congress of Mechanical Engineering (COBEM 2013)*, 2013.

[24] S. B. Shiki, S. da Silva, J.P. Noël, and G. Kerschen. Identification of a geometrically nonlinear beam using Volterra series. *Mechanics Research Communications*, Submetido para avaliação, 2013.

[25] Sidney Bruce Shiki, Cristian Hansen, and S. da Silva. Nonlinear features identified by Volterra series for damage detection in a buckled beam. In *International Conference on Structural Nonlinear Dynamics and Diagnosis - CSNDD 2014*, volume 16, Agadir, Morocco, May 2014.

[26] S. B. Shiki, Cristian Hansen, and S. da Silva. Parameter identification of a nonlinear beam with hardening behavior using Volterra series. In *5th Conference on Nonlinear Vibrations, Localization and Energy Transfer - NV2014*, Istanbul, Turkey, July 2014.